

3rd CIRP Global Web Conference

Feature extraction and pattern recognition in acoustic emission monitoring of robot assisted polishing

T. Segreto^{a,b,*}, S. Karam^{a,b}, R. Teti^{a,b}, J. Ramsing^c^aFraunhofer Joint Laboratory of Excellence on Advanced Production Technology (Fh J_LEAPT)^bDept. of Chemical, Materials and Industrial Production Engineering, University of Naples Federico II, Piazzale Tecchio 80, Naples 80125, Italy^cStrecon A/S, Stødagervej 5, DK-6400 Sønderborg, Denmark* Corresponding author. Tel.: +393471337695; fax: +390817682362. E-mail address: tsegreto@unina.it.**Abstract**

Polishing processes are to date gradually evolving from basically manual operations to automated processes. To achieve more accurate, steadfast and dependable automated polishing processes, sensor monitoring offers as a creditable tool for process and product quality control. In this study, an acoustic emission sensor monitoring system was employed for surface roughness assessment during robot assisted polishing of steel bars. After sensor signal pre-processing, feature extraction procedures were applied to the conditioned acoustic emission signals. The scope was to extract relevant signal features to input to pattern recognition paradigms in order to identify correlations between process generated acoustic emission and polished workpiece surface roughness.

© 2014 The Authors. Published by Elsevier B.V. This is an open access article under the CC BY-NC-ND license

[\(http://creativecommons.org/licenses/by-nc-nd/4.0/\)](http://creativecommons.org/licenses/by-nc-nd/4.0/).

Selection and peer-review under responsibility of the International Scientific Committee of the “3rd CIRP Global Web Conference” in the person of the Conference Chair Dr. Alessandra Caggiano.

Keywords: Polishing; Surface roughness; Sensor monitoring; Acoustic emission; Feature extraction; Pattern recognition**1. Introduction**

Surface finishing processes are widely used as the final step in the fabrication of a part in order to realise on it an extremely smooth surface [1]. At present, one of the most accurate surface finishing processes is polishing [2], defined as the process of creating a surface smoother than the one of the initial workpiece [3].

Polishing has traditionally been a manual process performed by skilled operators but becoming an automated process [4]. Polishing automation is a fundamental issue for process improvement in terms of required operational time and achieved surface quality. Robot assisted polishing (RAP) employs a robotic arm to perform polishing on a given workpiece [5].

To inspect the surface of a manufactured workpiece, surface metrology is traditionally based on tactile methods which gather data through physical contact with the surface [6]. This direct inspection method requires halting the polishing process to allow for dismounting

the workpiece and move it to the metrological instrument where surface roughness is measured.

Polishing sensor monitoring allows for product quality monitoring and process control in order to improve the solidness, dependability as well as the automation of manufacturing operations [7]. The most widely used sensors for polishing process monitoring are force, acoustic emission (AE), motor current, and vibrations, that can detect process relevant sensor signals to be further analysed. Feature extraction procedures need to be applied to the detected and conditioned sensor signals with the scope to provide a signal characterisation as concise as possible while maintaining the relevant information about process conditions [8].

The application illustrated in this study focuses on the improvement of the repeatability characteristics of a robot automated polishing process. For this purpose, an experimental campaign was carried out on a robot assisted polishing (RAP) machine developed by Strecon A/S [9] during polishing of AISI 52100 alloy steel under variable process conditions. During polishing, acoustic

AE raw signals were detected and conditioned, and feature extraction methodologies were applied to the conditioned signals: statistical analysis and wavelet packet transform (WPT) [10, 11]. The aim was to construct pattern feature vectors to be fed to neural network (NN) pattern recognition paradigms for correlating AE sensor signal features to polished workpiece surface roughness [12].

2. Experimental tests

Experimental polishing tests were conducted at Strecon A/S within the activities of the FP7 European project (FoF NMP – 285489) - Intelligent Fault Correction and self-Optimizing Manufacturing systems (IFaCOM) [13]. Strecon's RAP machine was utilized to polish 75 mm long cylindrical bars of AISI 52100 alloy steel (Fig. 1) with a Gesswein #800 polishing stone.

During the experimental tests, the polishing parameters were as follows:

- Main spindle rotational speed = 300 rpm
- Feed speed = 5 mm/s
- Polishing force = 1800 or 1000 g
- Oscillation = 500 pulses per min
- Stroke = 1 mm

Six polishing sessions, each composed of 60 passes, were carried out with session duration ~ 15 min and 50 s. During each polishing session, the full length of the alloy steel bar was polished over and over using alternated polishing force values:

- 1800 grams 1 × 60 passes
- 1000 grams 3 × 60 passes
- 1800 grams 2 × 60 passes

For each polishing session, AE raw signals were acquired using a Fuji Ceramics Corporation sensor (R-CAST M304A); they were then pre-amplified with A1002 AE pre-amplifier and digitised by an A/D board with sampling frequency 1 MHz. In Fig. 2, the RAP machine is shown with the AE sensor installed on it. A total number of 5580 AE digital signal files were obtained, each containing 131,072 AE signal samplings.



Fig. 1. Workpiece: AISI 52100 alloy steel bar



Fig. 2. Strecon's RAP machine with AE sensor and pre-amplifier

3. Roughness measurements

After each polishing session, the surface roughness values R_a , R_z and R_t (total height) [14] were measured on a Mahr profilometer by halting the polishing process and dismounting the workpiece. After measurement, the workpiece was re-mounted and the polishing process continued. The measured average surface roughness values are reported in Table 1 and plotted vs. polishing session number in Fig. 3.

Table 1. Surface roughness measurements (the final surface roughness measurement after session number 6 was not carried out).

Polishing session	Roughness values		
	R_a	R_z	R_t
1 (60 passes with 1800 g)	0.111	1.131	1.684
2 (60 passes with 1000 g)	0.081	0.984	1.582
3 (60 passes with 1000 g)	0.083	0.908	1.065
4 (60 passes with 1000 g)	0.053	0.603	0.742
5 (60 passes with 1800 g)	0.107	1.076	1.643
6 (60 passes with 1800 g)	N/A	N/A	N/A

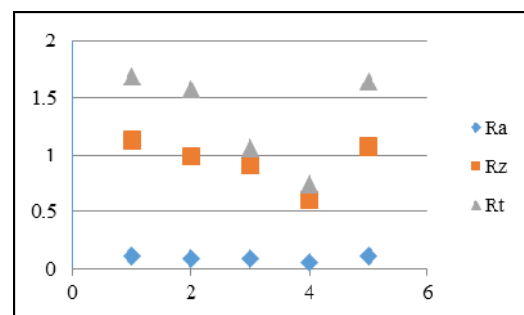


Fig. 3. Measured average surface roughness values vs. polishing session number.

4. AE signal pre-processing

AE raw signals typically oscillate around zero yielding a zero mean [15]. The acquired AE raw signals, however, showed a bias consisting in an offset likely due to electronic noise from the AE sensor system. A pre-processing phase was necessary to remove the bias by shifting the AE raw signals in order to achieve a zero mean signal, as illustrated in Fig. 4. For each AE raw signal (Fig. 4a), the signal average value was calculated and subtracted from the original signal to yield the typical AE raw signal oscillating around zero (Fig. 4b). Moreover, for each shifted AE raw signal, the root mean square (RMS) of the signal was evaluated with time constant 0.12 ms to provide the corresponding AE_{RMS} signal (Fig. 4c).

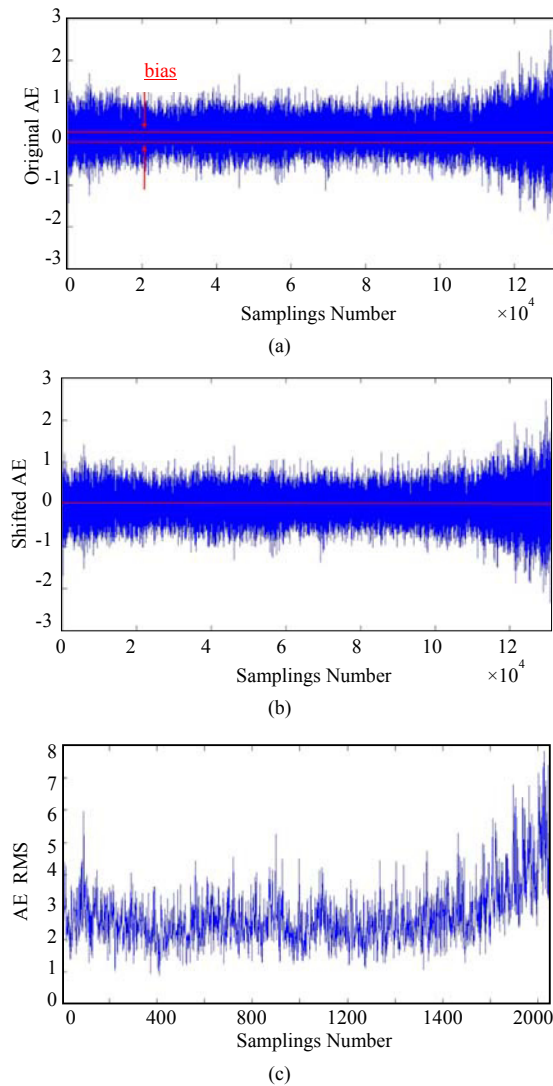


Fig. 4. (a) AE_{raw} signal; (b) AE shifted raw signal; (c) AE_{RMS} signal

5. AE signal feature extraction

The AE_{raw} and AE_{RMS} signals were subjected to diverse feature extraction procedures: (a) a conventional one based on statistical analysis feature extraction, and (b) an advanced one based on wavelet packet transform (WPT) feature extraction

5.1. Statistical analysis feature extraction

The signal mean, variance, skewness, kurtosis and energy were selected as statistical analysis features to be extracted from both the AE_{raw} and the AE_{RMS} signals [16]. These features made up the elements of statistical analysis pattern vectors to be inputted to pattern recognition paradigms for decision making on polished workpiece surface roughness acceptability. Fig. 5 shows the constructed statistical analysis pattern feature vectors for both the AE_{raw} and AE_{RMS} signals.

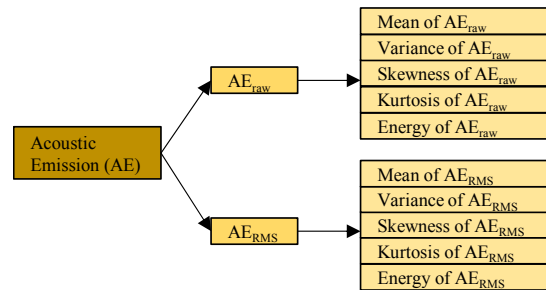


Fig. 5. Pattern vectors constructed with statistical analysis features from the AE_{raw} and AE_{RMS} signals.

5.2. Wavelet packet transform features extraction

The WPT of a signal generates packets of coefficients calculated by scaling and shifting a chosen mother wavelet, which is a prototype function. Accordingly, at the 1st level of the WPT, the original signal S is split into two frequency band packets called approximation, A_1 , and detail, D_1 . At the 2nd level, each approximation and detail packet are again split into further approximations, AA_2 and AD_2 , and details, DA_2 and DD_2 , and the process is repeated in the next levels generating other decomposition packets (Fig. 6) [17].

The mother wavelet employed for WPT of the AE_{raw} and AE_{RMS} signals is a Daubechies 3 denoted by "db3". The decomposition was performed up to the 3rd level yielding 14 packets. For each packet, 5 statistical features were calculated: mean, variance, skewness, kurtosis, and energy. To realize the WPT feature extraction procedure [18], a sensorial data table containing the n signals (5580 columns) composed of j digital signal samplings (131,072 rows) was created as shown in Fig. 7a.

As an example, the WPT feature extraction procedure for packet A is illustrated in Fig. 7. By applying the WPT to the 5580 AE signals, the corresponding 5580 A packets (columns) consisting of 65,540 coefficients (rows) were obtained (Fig. 7b). For each A packet, the five statistical features (mean, variance, kurtosis, skewness, energy) were calculated starting from its 65,540 coefficients (Fig. 7c). In Fig. 8, the constructed WPT pattern feature vectors for packet A are reported for the AE_{raw} and AE_{RMS} signals. Overall, $14 \text{ packets} \times 2 \text{ AE signal types} = 28$ total WPT pattern feature vectors were obtained. These WPT pattern feature vectors were utilised as inputs to cognitive pattern recognition paradigms for decision making on polished workpiece surface roughness acceptability.

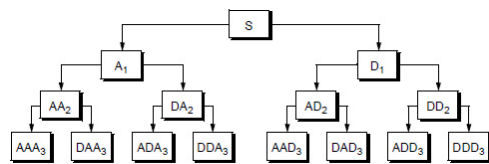


Fig. 6. WPT 3rd level decomposition tree.

Signal ID	1	2	5580
Samplings			
1	2.85×10^2	4.09×10^2	-6.11
2	3.68×10^2	4.25×10^2	6.11
...
131072	3.78×10^2	4.43×10^2	6.04×10^2

(a) Sensorial Data

Signal ID	1	2	5580
Coeff. of Packet A			
1	2.85×10^2	4.09×10^2	-6.11
2	3.68×10^2	4.25×10^2	6.11
...
65540	3.78×10^2	4.43×10^2	6.04×10^2

(b) Coefficient of the A packet

Feat. for Packet A	Mean	Var	Skew	Kurt	Energy
1	5.453	488.52	2322.2	1050.8	112
...
5580	4.873	325.12	2557.4	972.1	88

(c) Five elements WPT statistical feature vectors

Fig. 7. WPT feature extraction procedure for packet A

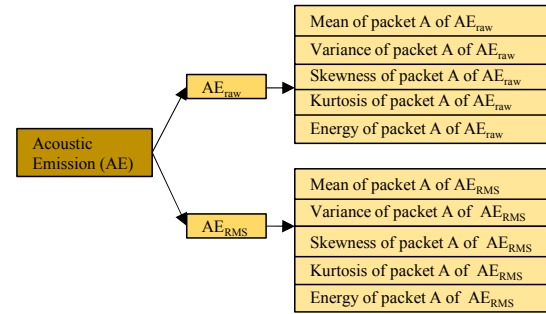


Fig. 8. Pattern vectors constructed with WPT features from the AErAw and AERMS signals.

6. Neural network based decision making

The statistical analysis and WPT pattern feature vectors extracted from the conditioned AE signal types were utilised as inputs to decision making paradigms based on neural network (NN) data processing [19].

A three-layer NN configuration [20] was implemented for each of the 30 input pattern feature vectors: 28 WPT pattern feature vectors and 2 statistical analysis pattern feature vectors. The NN architecture was 5-15-1 with 5 nodes in the input layer receiving the 5 features of each pattern vector, 15 nodes in the hidden layer related to the number of input nodes, and 1 node in the output layer providing a binary target value associated to surface roughness acceptability: "0" for acceptable surface roughness, and "1" for unacceptable surface roughness.

The NN training set was built up by mating the correct binary target value to each of the 5580 AE digital signal files in order to map the input sensor signal pattern feature vector to the output surface roughness acceptability assessment. This was realised as follows: the measured R_a values were linearly connected (see Fig. 12) and a threshold for surface roughness acceptability was set at $R_a = 0.07 \mu\text{m}$, representing the roughness required from the polishing process. Sensor signal files corresponding to a linearly interpolated $R_a \leq 0.07 \mu\text{m}$ were coupled with a "0" binary output, i.e. acceptable surface roughness, and sensor signal files corresponding to a linearly interpolated $R_a > 0.07$ were coupled with a "1" binary value, i.e. unacceptable surface roughness.

The output of the NN decision making paradigm is composed of a set of percentages called success rates (SR): training set SR, validation set SR, testing set SR, and overall SR. The most relevant for NN performance evaluation is the overall SR, defined as the percentage of successful classification cases that the NN has achieved in relating the input data to the desired output [21, 22].

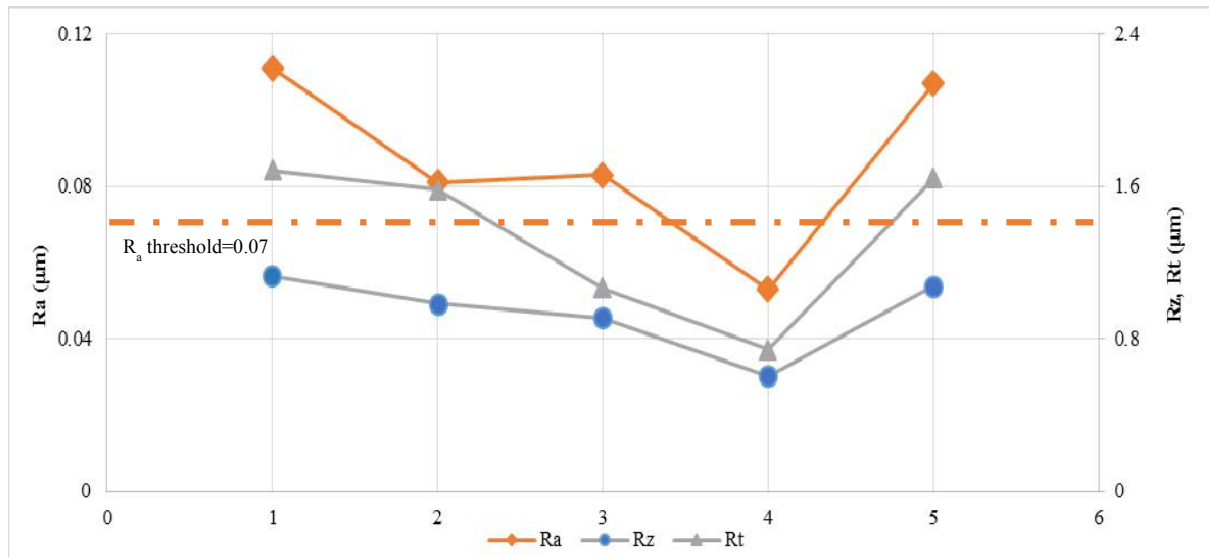


Fig. 9. Broken straight lines: measured roughness values graphs. Horizontal dotted lines: minimum and maximum Ra threshold levels.

7. Results and discussion

The NN overall SR values for each of the statistical analysis and WPT input pattern feature vectors, for both the AE_{raw} and AE_{RMS} signals, are reported in Table 2.

As regards the behaviour of the statistical analysis pattern feature vectors, both the AE_{raw} and AE_{RMS} signal feature patterns provided interestingly high SR values, with the AE_{RMS} signal SR = 79.25% slightly higher than the AE_{raw} signal SR = 78.76% (Table 2).

As for the WPT pattern feature vectors, their performance was in all cases higher than for the statistical analysis pattern feature vectors, always yielding SR values > 81% (Table 2). In this case, the AE_{raw} signal allowed to achieve higher NN performances than the AE_{RMS} signal: the average and maximum SR values for the WPT pattern feature vectors for AE_{raw} signals (SR_{ave} = 84.17%, SR_{max} = 86.69% for the ADA packet) were higher than those for AE_{RMS} signals (SR_{ave} = 83.32%, SR_{max} = 85.47% for the DDA packet) (Fig. 13). The obtained classification results suggest a generally higher capability of the WPT methodology in making full use of the available sensorial information, the more so in the case of the heftier AE_{raw} signal.

8. Conclusion

Sensor monitoring technology was employed during automated polishing of steel bars in order to detect sensor signals from which to extract process relevant

features with the purpose to relate them to the polished workpiece surface roughness acceptability.

Based on effectual sensory data analysis and reliable decision making, the polishing process can be halted when the required surface roughness is achieved in order to avoid overpolishing that is detrimental for the polished surface quality.

A sensor monitoring experimental campaign was carried out on Strecon's robot assisted polishing (RAP) machine where an acoustic emission (AE) sensor was installed. The polished steel bar surface roughness was measured after a pre-defined number of passes set up in the testing programme. The detected AE raw signals were pre-processed and two types of conditioned signals were considered for analysis: AE_{raw} and AE_{RMS} signals. From the conditioned signals, relevant features were extracted using diverse signal processing methodologies: statistical analysis and wavelet packet transform (WPT).

The extracted features were used to construct pattern feature vectors to feed to neural network (NN) based pattern recognition paradigms for decision making on polished workpiece surface roughness acceptability. By considering the NN success rate (SR) obtained using the two procedures of feature extraction from both AE signal types, it can be stated that each of the two techniques provide interestingly high SR performance for both kinds of conditioned signals. A generally higher capability of the WPT methodology in making full use of the available sensorial information can be observed, the more so in the case of the heftier AE_{raw} signal.

Table 2. Overall NN SR for all 30 input pattern feature vectors (threshold = 0.07)

AE _{raw} sensor signals		AE _{RMS} sensor signals	
NN SR (%)		NN SR (%)	
Statistical features	78.76	Statistical features	79.25
WPT pattern feature vectors		WPT pattern feature vectors	
A	84.23	A	82.23
D	83.45	D	83.31
AA	84.98	AA	81.13
DA	83.44	DA	83.35
AD	81.89	AD	82.82
DD	83.74	DD	82.23
AAA	85.38	AAA	85.21
DAA	83.56	DAA	82.12
ADA	86.69	ADA	84.56
DDA	84.34	DDA	85.47
AAD	83.65	AAD	83.23
DAD	85.52	DAD	84.65
ADD	82.24	ADD	82.88
DDD	85.25	DDD	83.34
SR average	84.17	SR average	83.32

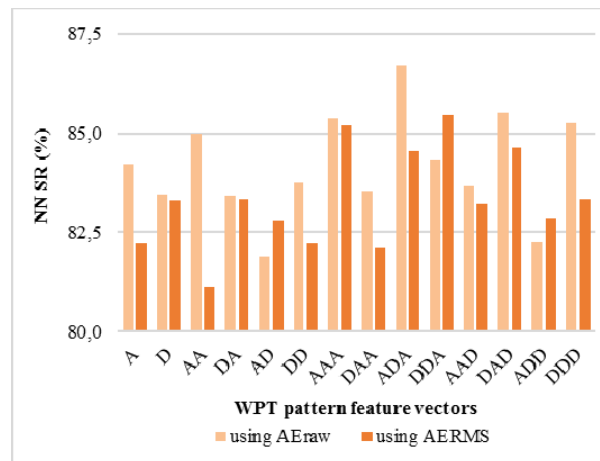


Fig. 10. Overall NN SR for the WPT input feature pattern vectors

References

- [1] Evans, C.J., Paul, E., Dornfeld, D., Lucca, D.A., Byrne, G., Tricard, M., Klocke, F., Dambon, O., Mullany, B.A., 2003. Material removal mechanisms in lapping and polishing, CIRP Annals, 52/ 2, p. 611.
- [2] Marinescu, I., Uhlmann, E., Doi, T., 2006. Handbook of Lapping and Polishing, CRC Press, Taylor & Francis Group.
- [3] <http://en.wikipedia.org/wiki/Polishing>. Retrieved on 20/05/2014.
- [4] Rebeggiani, S., Rosén, B. G., 2011. High gloss polishing of tool steels – step by step. Proc. of the 4th Swedish Production Symposium, Sweden, Lund, p. 257.
- [5] <http://www.strecon.com/Robot-Assisted-Polishing-82.aspx> Retrieved on 20/05/2014.
- [6] Li, F., Longstaff, A. P., Fletcher, S., Myers, A., 2012. Integrated tactile and optical measuring systems in three dimensional metrology. Proc. of the Computing and Engineering Annual Researchers' Conf. 2012, University of Huddersfield, p. 1.
- [7] Pilný, L., Bissacco, G., De Chiffre, L., Ransing, J., 2013. Acoustic emission based in-process monitoring in robot assisted polishing. The 11th International Symposium of Measurement Technology and Intelligent Instruments, p. 1.
- [8] Teti, R., Jemielniak, K., O'Donnell, G., Dornfeld, D., 2010. Advanced monitoring of machining operations, CIRP Annals, 59/2, p. 717.
- [9] <http://www.strecon.com/>
- [10] S. Karam, R. Teti, 2013. Wavelet Transform Feature Extraction for Chip form Recognition during Carbon Steel Turning, Procedia CIRP 12, p. 97.
- [11] Jemielniak, K., Teti, R., Kossakowska, J., Segreto, T., 2006. Innovative Signal Processing for Cutting Force Based Chip form Prediction, Intelligent Production Machines and Systems - 2nd I*PROMS Virtual International Conference, p. 7.
- [12] Hertz J, Krogh A, Palmer RG, 1991. Introduction to the theory of neural computation. Addison-Wesley, New York.
- [13] EC FP7, Call for FoF, Towards Zero-Defect Manufacturing, 2011-NMT-ICT-FoF, Intelligent Fault Correction and Self Optimising Manufacturing Systems - IFaCOM (2011-15).
- [14] Exploring Surface Texture: A fundamental guide to the measurement of surface finish. 7th ed. 2011. Taylor Hobson, UK.
- [15] Beattie, A. G., 1979, Studies in the digital analysis of acoustic emission signals. In Kanji Ono ed., Fundamentals of Acoustic Emission, University of California LA, p. 17.
- [16] Segreto, T., Simeone, A., Teti, R., 2013. Multiple sensor monitoring in nickel alloy turning for tool wear assessment via sensor fusion, Procedia CIRP 12, p. 85.
- [17] Misiti, M., Misiti, Y., Oppenheim, G., Poggi, J.M., 1996. "Wavelet Toolbox for Use with Matlab", Version 1.
- [18] Segreto, T., Karam, S., Simeone, A., Teti, R., 2013. Residual stress assessment in Inconel 718 machining through wavelet sensor signal analysis and sensor fusion pattern recognition, Procedia CIRP 9, p. 103.
- [20] Jordan, M.I., Bishop, C.M., 2004. "Neural Networks". In Allen B. Tucker. Computer Science Handbook, Second Edition (Section VII: Intelligent Systems). Boca Raton, FL: Chapman & Hall/CRC Press LLC.
- [21] Segreto, T., Simeone, A., Teti, R., 2012. Sensor fusion for tool state classification in nickel superalloy high performance cutting. Procedia CIRP 1, p. 593.
- [22] Segreto, T., Simeone, A., Teti, R., 2014. Principal component analysis for feature extraction and NN pattern recognition in sensor monitoring of chip form during turning, CIRP Journal of Manufacturing Science and Technology 7, p. 202.